

Noncovalent functionalization of few-layer black phosphorus with metal nanoparticles and its application in catalysis

Maria Caporali,^{a,*} Manuel Serrano-Ruiz,^a Francesca Telesio,^b Stefan Heun,^b Giuseppe Nicotra,^c Corrado Spinella,^c Stefano Caporali,^{d,e} Maurizio Peruzzini^{a,*}

^a CNR-ICCOM, Via Madonna del Piano 10, 50019 Sesto Fiorentino, Italy.

^b NEST, Istituto Nanoscienze-CNR e Scuola Normale Superiore, Piazza S. Silvestro 12, 56127 Pisa, Italy.

^c CNR-IMM, Istituto per la Microelettronica e Microsistemi, Strada VIII, 5, 95121 Catania, Italy.

^d Consorzio INSTM, Dipartimento di Chimica, Università degli Studi di Firenze, Via della Lastruccia 3, 50019 Sesto Fiorentino, Italy.

^e CNR-ISC, Via Madonna del Piano 10, 50019 Sesto Fiorentino, Italy.

Abstract

Transition metal nanoparticles of Ni, Pd, Ru and Au, each of them stabilized by a suitable capping agent, were dispersed on the surface of few-layer black phosphorus (2D BP) achieving new nanocomposite 2D materials. Ni nanoparticles supported on 2D BP worked successfully in the hydrogenation of phenylacetylene, showing good catalytic activity preserved after recycling tests. These results highlight that 2D BP is able to stabilize metal nanoparticles through weak noncovalent interactions and disclose a wide application of 2D BP as a hosting platform for catalytically active metal species.

Black phosphorus (BP) has a layered structure analogue to graphite and lately it has been shown that, following a similar procedure to bulk graphite, it can be exfoliated down to the monolayer. In this way, a new member of the growing family of 2D materials, named phosphorene,^{1,2} being the all P-counterpart of graphene, was isolated. Single and few-layer BP (2D BP) have been obtained by either micromechanical cleavage (Scotch tape method)³ or liquid exfoliation.⁴ In our labs, good quality phosphorene flakes were prepared by sonicating BP microcrystals in dimethylsulfoxide (DMSO) keeping an inert atmosphere and in the dark.⁵ Since its discovery, the new P-based 2D material attracted an enormous interest, as it is endowed with a direct and tunable band gap ranging from 0.3 eV (bulk) to 2.0 eV (monolayer), a high on/off ratio ($>10^5$), and a high carrier mobility (up to $1000 \text{ cm}^2\text{V}^{-1}\text{s}^{-1}$) which prompted its application towards the production of nano-electronic devices, as for instance FETs (field effect transistors).⁶ In spite of this huge interest, only an handful

of reports have dealt with the surface functionalization of 2D BP so far,⁷ while many theoretical studies have been carried out indicating that a wide range of chemical reactions of this new and fascinating material are prone to be explored. Based on first-principles calculations, a systematic study on the binding energy, geometry, magnetic moment, and electronic structure of several metal ad-atoms adsorbed on phosphorene has been carried out,⁸ predicting that the immobilization of transition metals on the surface of phosphorene is feasible, while preserving its structural integrity. Indeed, the lone pair available on each trivalent phosphorus atoms forming the BP layer, should impart a soft Lewis base character, reclaiming a straightforward reactivity towards a soft Lewis acid molecule, such as a late-transition metal.⁹ On these basis, we were curious to verify experimentally the behavior of exfoliated BP towards late-transition metal nanoparticles. Two methods were followed to achieve this goal; the first was based on a biphasic system and the second used a homogeneous phase. In the first approach, a colloidal solution of nickel nanoparticles in *n*-hexane stabilized by trioctylphosphine was prepared¹⁰ and mixed with 2D BP suspended in DMSO. In few minutes, the nanoparticles underwent a net phase-transfer moving to the DMSO phase that immediately changed color from originally brownish-yellow to black while the *n*-hexane phase faded completely. The second procedure was carried out by mixing 2D BP suspended in tetrahydrofuran (THF) with Ni NPs dispersed in toluene. The synthetic procedure worked out well also using different P:Ni molar ratios, 12:1, 6:1, and 2:1. Conventional bright field TEM analysis showed well dispersed nickel nanoparticles on the surface of 2D BP, see Figure 1. After their immobilization, Ni nanoparticles preserved their size, average diameter of 12 nm, and no aggregation took place.

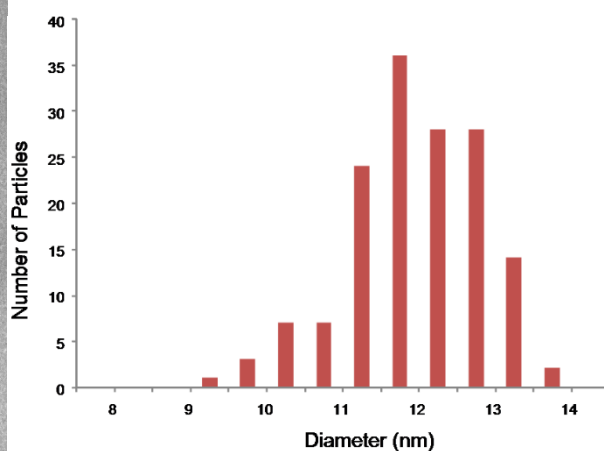
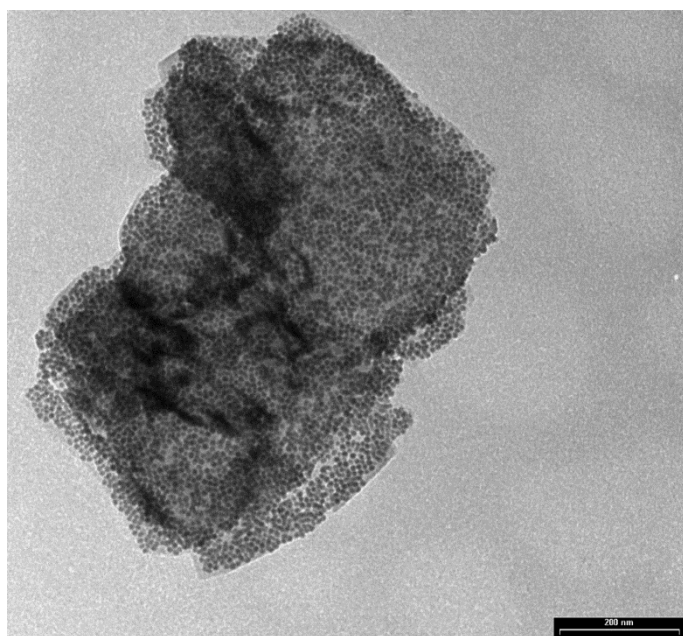


Figure 1. Left: bright field TEM image of nickel nanoparticles supported on few-layer black phosphorus. Scale bar: 200 nm. Right: size distribution of the nickel nanoparticles. P:Ni molar ratio 2:1.

EDX performed on different points of the same sample confirmed the chemical identity of the 2D material, see Figure S1, and corroborated the presence of Ni on the surface of 2D BP.

Afterwards, high angle annular dark field (HAADF) STEM was carried out to study the sample at the atomic level, see below Figure 2.

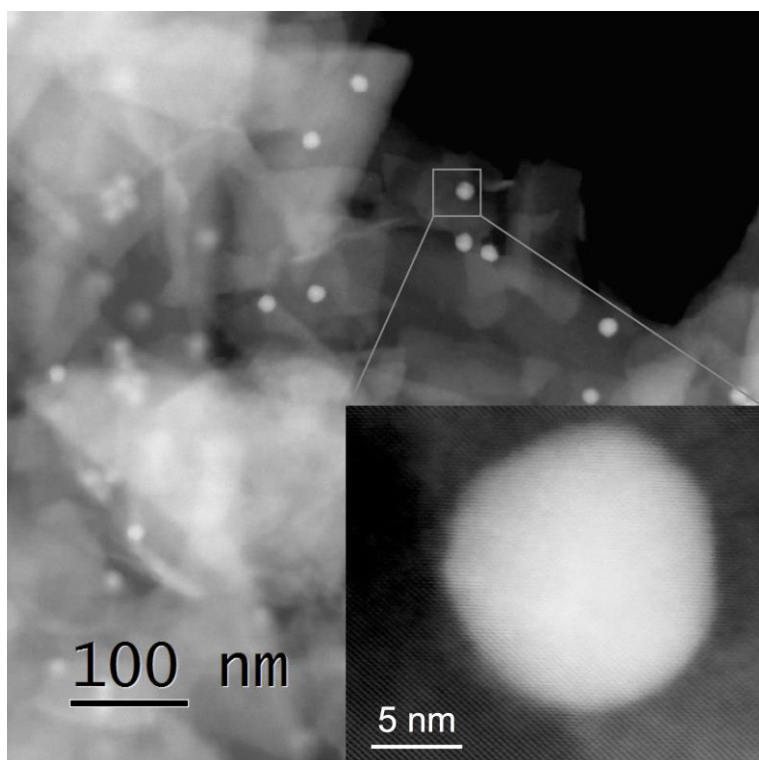


Figure 2. HAADF-STEM of Ni NPs -2D BP with inset at atomic resolution.

By the combination of STEM and EELS analysis technique named spectrum imaging (SI)¹¹ we may disclose the chemical composition of the surface of the new nanocomposite. On this purpose, we acquired the experimental Ni $L_{2,3}$ -edge energy loss near edge structure (ELNES), for Ni NPs and NiO NPs, grey and red spectra on Figure 3 respectively, and compared with the ones found on literature, blue and purple respectively.¹² Our EELS spectra shown in Figure 3, were extracted from the SI dataset after background subtraction and multiple scattering deconvolution, in order to avoid artifact due to the thickness. Here, besides the L_3 and L_2 peaks at 855eV and 872eV, respectively, a secondary peak is observed at about 7-8 eV energy from the main Ni L_3 -edge (see arrow on grey spectrum). This secondary peak is present only in pure Ni and metallic compounds¹² and arises from a 4p-4d hybridized band¹² that is absent in nickel oxide (see arrow on red spectrum). These

results, compared with the spectrum acquired on NiO NPs, showing a typical bump around 869eV¹² (see black arrow on red and purple spectra of Figure 3), provide strong confirmatory evidence that the BP flakes are decorated with pure metallic nickel nanoparticles.

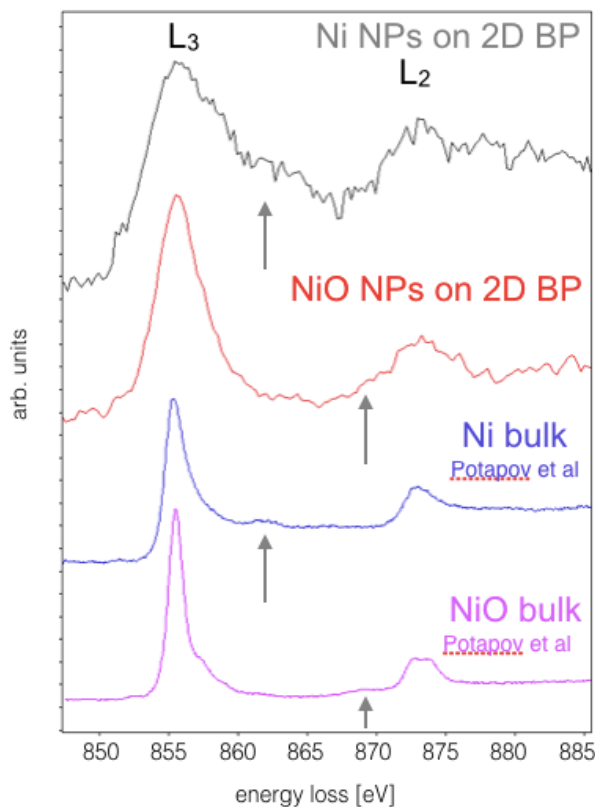


Figure 3. Ni L_{2,3}-edge Energy Loss Near Edge Structure (ELNES) for Ni NPs/2D BP and NiO NPs, and the equivalent signals from bulk structures of Ni and NiO.¹²

A Raman spectroscopy study was carried out to further characterize the new 2D material.¹³ Thus, Figure 4 compares the Raman spectrum of a freshly prepared sample of 2D BP (blue curve) with the same batch of 2D BP after functionalization with nickel nanoparticles (red curve). The spectrum of the nickel functionalized material reveals the three typical Raman bands of phosphorene at 360 cm⁻¹, 435 cm⁻¹, and 460 cm⁻¹, attributed to the A_g¹, B_{2g}, and A_g² vibrational modes, respectively.¹⁴ The lack of differences in both the Raman shift and intensity ratio between the two spectra in Figure 4 suggests the absence of any strong covalent interaction, *i.e.* a chemical bond, between the nickel nanoparticles and the P-atoms of the 2D BP support.¹⁵

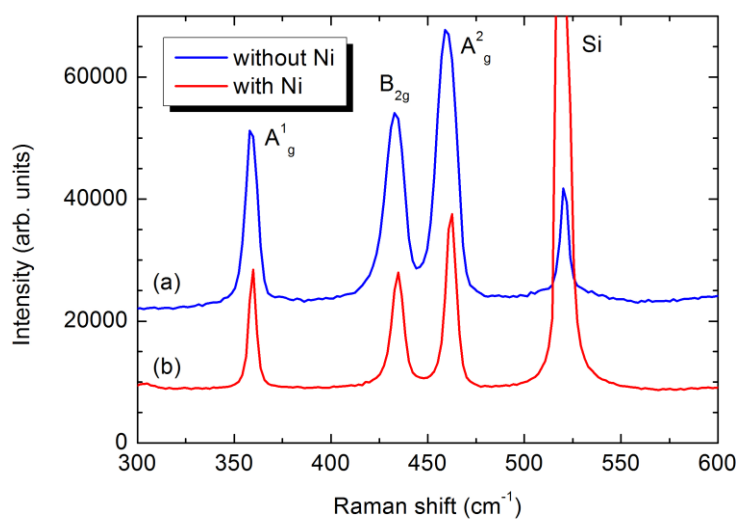


Figure 4. Comparison of the Raman spectra between a) blue curve: pristine few-layer BP; b) NiNPs/2D BP. The strong peak at 520 cm^{-1} is due to the silicon substrate.

Transition metals other than nickel may be used to prepare different phosphorene nanocomposites, following the same strategy mentioned above. Thus, a colloidal solution of Ru nanoparticles stabilized with oleylamine¹⁶ (average diameter: 2.4 nm), Pd nanoparticles stabilized with tetraoctyl ammonium bromide¹⁷ (average diameter 2.8 nm), and Au nanoparticles stabilized by dodecanethiol¹⁸ (average diameter 6.5 nm), were each separately added to a suspension of 2D BP as described in the Supporting Info. The morphological analysis of the nanocomposites resulting from the immobilization of metal nanoparticles on 2D BP was carried out by TEM, see Figures S2-S4, showing that the nanoparticles were always well dispersed on the surface of BP. Especially for Ni and Ru, a high dispersability of the nanoparticles on the surface was observed, and a molar ratio phosphorus:metal as high as 2:1 could be used. When this ratio was used for Pd NPs and Au NPs, TEM inspection showed a large amount of un-supported nanoparticles. Therefore, in a second experiment a lower molar ratio P:metal of 15:1 was used, and this time no free colloidal nanoparticles were detected by TEM. Raman characterization was carried out for all the nanocomposites, see Figures S5-S7 and, as for nickel, no appreciable differences with pristine phosphorene were observed, meaning the absence of a strong covalent interaction between the metal nanoparticles and 2D BP. UV-Vis spectra were registered on the nickel and on the gold nanocomposite and a comparison with UV-Vis spectra of pristine 2D BP and free colloidal nanoparticles is shown in Figure S8. Interestingly, the surface plasmon resonance of Au nanoparticles shifted from 502 nm to 540 nm once they were dispersed on 2D BP and the band appears much broader. This red shift may be due to the interaction between gold nanoparticles and

the surface of 2D BP. It is indeed observed in several composites, as AuNPs/TiO₂¹⁹ and AuNPs on graphene oxide,²⁰ the broadening and shifting of the plasmon band.

Measurements of the P 2p core-level photoemission spectra were carried out on both pristine phosphorene and on the nanocomposite bearing gold nanoparticles. In Figure 5, the freshly prepared few layer-black phosphorus presents the 2p_{3/2} and 2p_{1/2} doublet at 129.7 eV and 130.5 eV, respectively, characteristic of crystalline black phosphorus,⁴ confirming that the 2D BP is completely un-oxidized. The chemical purity of our exfoliated BP was also checked by STEM-EELS, see Figure S9.

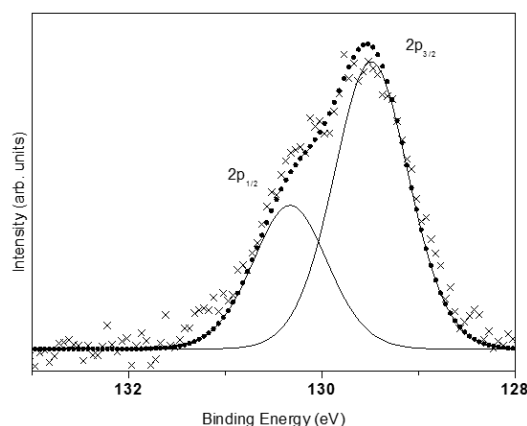


Figure 5. Deconvoluted XPS P 2p spectrum of pristine 2D BP. Raw data are represented by cross symbols (x), dashed lines represent the 2p_{1/2} and 2p_{3/2} components, and full circles represent the envelope spectrum.

The left side of Figure 6 shows the Au 4f XPS spectrum of Au NPs immobilized on the surface of 2D BP, with the doublet at 84.0 and 87.7 eV referring to Au 4f_{7/2} and Au 4f_{5/2} respectively, characteristic of metallic gold. There is a relatively small contribution (10% roughly) due to gold in oxidation state +1, as shown by the doublet at 85.7 and 89.4 eV. The right side of Figure 6 shows the P 2p_{3/2} and P 2p_{1/2} doublet at 130.2 eV and 131.1 eV, respectively, characteristic of elemental black phosphorus, indicating that the surface of phosphorene remains completely un-oxidized after the deposition of the metallic nanoparticles. In comparison to Figure 5, which refers to pristine 2D BP, we observe here only a very minor shift in the P 2p doublet, suggesting a weak interaction between the support and the gold nanoparticles. The C 1s XPS spectrum of Au NPS/2D BP is shown in Figure S10, where the peak at the binding energy of 285 eV is characteristic of organic carbon and reasonably due to the capping agent, *i.e.* dodecanethiol, which covers the surface of gold nanoparticles.

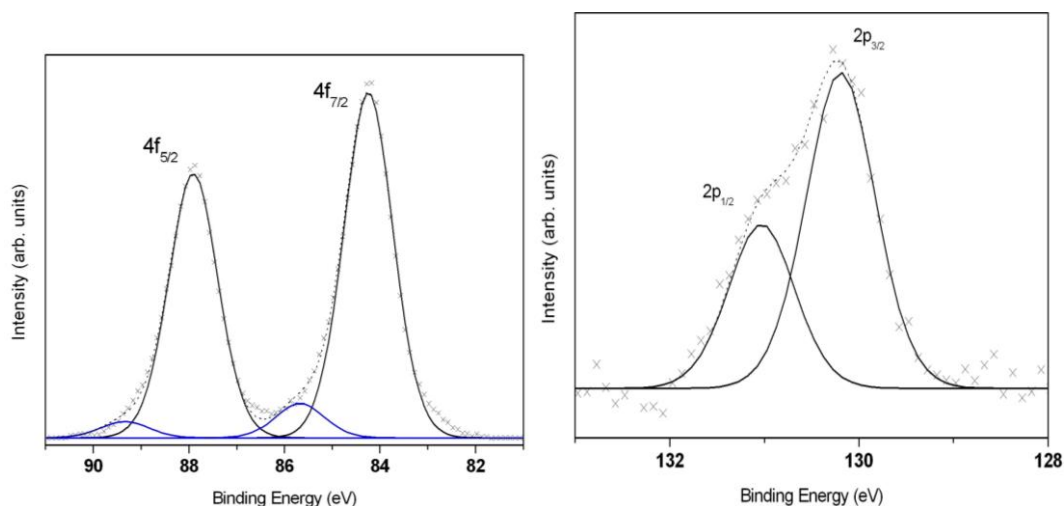
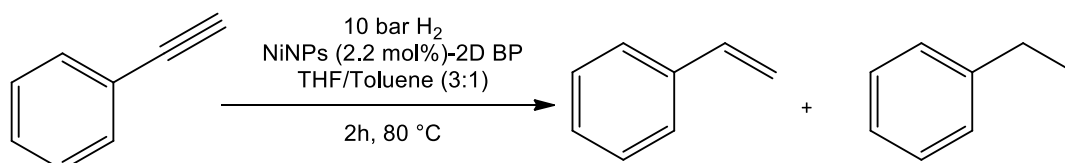


Figure 6. Curve fitting of the Au 4f (left side) and P 2p (right side) XPS spectra of AuNPs/2D BP.

As a benchmark test, the hydrogenation of phenylacetylene catalysed by Ni NPs/2D BP was studied. The heterogeneous catalyst was prepared as detailed in the Supporting Info.



Scheme 1. Hydrogenation of phenylacetylene catalyzed by Ni NPs supported on 2D BP.

The conversion was quantitative with high selectivity towards styrene, see Table 1, run 0. Reusability of the heterogeneous catalyst was tested and the conversion was quantitative until the third recycling test. In comparison, free colloidal nickel nanoparticles showed lower stability, being inclined to oxidize easily, with conversion rates which may drop significantly even after one run.²¹ In our case, TEM inspection of Ni NPs/2D BP recovered after the catalytic tests confirmed the presence of nickel nanoparticles only on the surface of the nanosheets and their mean dimension still around 12 nm as before starting the catalysis, see Figure S11.

Run	Conversion (%)	Selectivity to styrene(%)*
0	100.0	87.6 (12.4)
1	100.0	88.5 (11.5)
2	100.0	92.2 (7.8)
3	99.2	93.1 (6.1)

*in brackets the percentage of ethylbenzene.

Table 1. Recycling tests. Reaction conditions: 10 bar H₂, 80 °C, 2 hours, Ni NPs/2D BP = 2.2 mol %, THF : toluene (3:1), total volume: 1.6 mL. Both conversion and selectivity were evaluated by GC analysis.

To verify the behavior of the system in the conditions used for the catalysis, DLS measurements were run on the nanocomposite Ni NPs/2D BP both at room temperature and at T = 80 °C. Interestingly, no free colloidal particles were observed once the sample was heated up, see Figure S13. Only a reduction of the mean size, from 747.1 nm (measure at RT, Figure S12) to 395.3 nm, was observed, which is reversible when the sample is cooled back to 25°C, with a mean size of 776.7 nm, see Figure S14. In keeping with this finding, the interaction between 2D BP and the metal nanoparticles is enough strong to survive along the catalytic conditions, thus making 2D BP a potentially good catalytic support.²²

In summary, due to its large surface area 2D BP has been shown for the first time to be a suitable support for the dispersion of transition metal nanoparticles of Ni, Ru, Pd, and Au. The nanocomposite Ni NPs/2D BP was tested in the hydrogenation of phenylacetylene and exhibited good catalytic activity that remained unaltered after recycling tests, showing that 2D BP plays a key role in the stabilization of nickel nanoparticles. The impact of nanocomposites produced by decorating exfoliated BP with metallic nanoparticles has promising important applications in several frontier research areas including photocatalysis, chemical sensors and energy storage.

Acknowledgments

Thanks are expressed to EC for funding the project PHOSFUN “*Phosphorene functionalization: a new platform for advanced multifunctional materials*” (ERC ADVANCED GRANT to M.P).

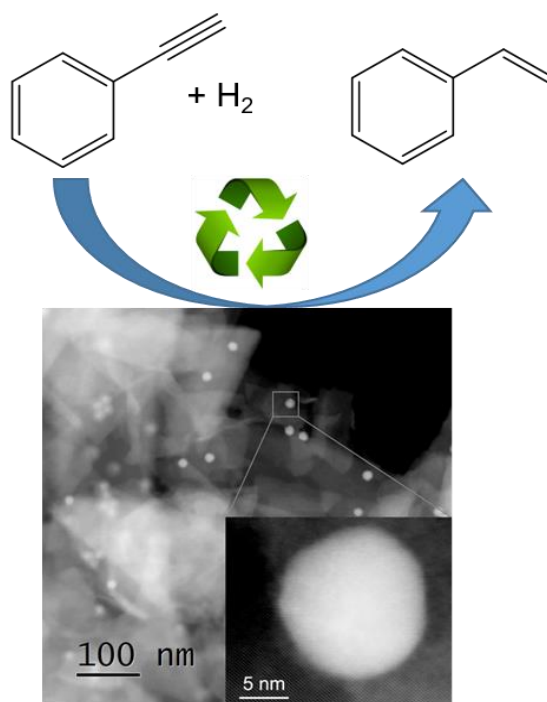
Part of this work was performed at Beyondnano CNR-IMM, which is supported by the Italian Ministry of Education and Research (MIUR) under project Beyond-Nano (PON a3_00363).

Keywords: black phosphorus, catalysis, functionalization, 2D materials, metal nanoparticles

Table of Contents

Metal nanoparticles of nickel, palladium, ruthenium and gold, each of them stabilized by a suitable capping agent, were dispersed on the surface of few-layer black phosphorus (2D BP) achieving new nanocomposite 2D materials. Ni nanoparticles supported on 2D BP worked successfully in the hydrogenation of phenylacetylene and showed good catalytic activity preserved after recycling

tests. Our work shows 2D BP as a hosting platform for catalytically active metal species thus paves the wide application few-layer BP in heterogeneous catalysis.



¹ a) E.S. Reich, *Nature* **2014**, *506*, 19; b) H.O.H. Churchill, P. Jarillo-Herrero, *Nature Nanotechnol.* **2014**, *9*, 330-331.

² a) L. Kou, C. Chen, S. C. Smith, *J. Phys. Lett.* **2015**, *6*, 2794-2805; b) S. Balendhran, S. Walia, H. Nili, S. Sriram, M. Bhaskaran, *Small* **2015**, *11*, 640-652.

³ a) K. Li, Y. J. Yu, G. J. Ye, Q. Q. Ge, X. D. Ou, H. Wu, D.L. Feng, X.H. Chen, Y.B. Zhang, *Nat. Nanotechnol.* **2014**, *9*, 372-377; b) H. Liu, A.T. Neal, Z. Zhu, Z. Luo, X. Xu, D. Tomanek, P.D. Ye, *ACS Nano* **2014**, *8*, 4033-4041.

⁴ a) S. C. Warren, A. H. Woomer, R. A. Wells, T. W. Farnsworth, US Patent appl. 62/031, 184, **2014**; b) J. Kang, D. Wood, S. A. Wells, D. Jariwala, K. S. Chen, E. Cho, V. K. Sangwan, X. Liu, L.J. Lauhon, T. J. Marks, M. C. Hersam, *Nano Lett.* **2014**, *14*, 6964-6970; c) J. Kang, J. D. Wood, S. A. Wells, J.-H. Lee, X. Liu, K.-S. Chen, M. C. Hersam, *ACS Nano*, **2015**, *9*, 3596-3604; d) P. Yasaei, B. Kumar, T. Foroozan, C. Wang, M. Asadi, D. Tuschel, J. E. Indacochea, R. F. Klie, A. Salehi-Khojin, *Adv. Mater.* **2015**, *27*, 1887-1892; e) A.H. Woomer, T.W. Farnsworth, J. Hu, R.A. Wells, C.L. Donley, S.C. Warren, *ACS Nano*, **2015**, *9*, 8869-8884; f) H. Wang, X. Yang, W. Shao, S. Chen, J. Xie, X. Zhang, J. Wang, Y. Xie, *J. Am. Chem. Soc.* **2015**, *137*, 11376-11382; g) Z. Guo, H. Zhang, S. Lu, Z. Wang, S. Tang, J. Shao, Z. Sun, H. Xie, H. Wang, X-F. Yu, P.K. Chu, *Adv.*

-
- Funct. Mater.* **2015**, *25*, 6996-7002; h) W. Zhao, Z. Xue, J. Wang, J. Jiang, X. Zhao, T. Mu, *ACS Appl. Mater. Interfaces* **2015**, *7*, 27608-27612; i) J. N. Coleman *et al.*, *Nat. Commun.* **2015**, *6*, 8563.
- ⁵ M. Serrano-Ruiz, M. Caporali, A. Ienco, V. Piazza, S. Heun, M. Peruzzini, *Adv. Mater. Interfaces*, **2016**, *3*, 1500441.
- ⁶ a) H. O. H. Churchill, P. Jarillo-Herrero, *Nat. Nanotechnol.*, **2014**, *9*, 330-331; b) S. Das, W. Zhang, M. Demarteau, A. Hoffmann, M. Dubey, A. Roelofs, *Nano Lett.* **2014**, *14*, 5733-5739; c) V. Tran, R. Soklaski, Y. Liang, L. Yang, arXiv:1402.4192v3 [cond-mat.mes-hall]; d) A. Castellanos-Gomez, *J. Phys. Chem. Lett.* **2015**, *6*, 4280-4291.
- ⁷ a) H.U. Lee, S.C. Lee, J. Won, B-C Son, S. Choi, Y. Kim, S. Y. Park, H-S Kim, Y-C Lee, J. Lee, *Sci. Rep.* **2015**, *5*, 8691-8697; b) Y. Zhao, H. Huang, Q. Xiao, Y. Hu, Z. Guo, H. Xie, J. Shao, Z. Sun, W. Han, X.F. Yu, P. Li, P. K. Chu, *Angew. Chem. Int. Ed.* **2016**, *55*, 5003-5007; c) C. R. Ryder, J. D. Wood, S. A. Wells, Y. Yang, D. Jariwala, T. J. Marks, G. C. Schatz, M. C. Hersam, *Nature Chem.* **2016**, *8*, 597-602.
- ⁸ a) V. V. Kulish, O. I. Malyi, C. Persson, P.Wu, *Phys. Chem. Chem. Phys.* **2015**, *17*, 992-1000; b) T.Hu, J. Hong, *J. Phys. Chem C* **2015**, *119*, 8199-8207; c) Y. Jing, X. Zhang, Z. Zhou, *WIREs Comput. Mol. Sci.* **2016**, *6*, 5-19; d) P. Rastogi, S. Kumar, S. Bhowmick, A. Agarwal, Y. S. Chauhan, arXiv:1503.04296v2 [cond-mat.mes-hall]; e) L. Seixas, A. Carvalho, A. H. Castro-Neto, *Phys. Rev. B* **2015**, *91*, 155138(1)-155138(6); X. Sui, C. Si, B. Shao, X. Zou, J. Wu, B.L. Gu, W. Duan, *J. Phys. Chem. C* **2015**, *119*, 10059-10063; f) H. Wang, S. Zhu, F. Fan, Z. Li, H. Wu, *J. Magnetism and Magnetic Mat.* **2016**, *401*, 706-710.
- ⁹ R.G. Parr, R.G. Pearson, *J. Am. Chem. Soc.* **1983**, *105*, 7512.
- ¹⁰ S. Carenco, C. Boissière, L. Nicole, C. Sanchez, P. Le Floch, N. Mézailles, *Chem. Mater.* **2010**, *22*, 1340-1349.
- ¹¹ G. Nicotra, Q. M. Ramasse, I. Deretzis, A. La Magna, C. Spinella, F. Giannazzo, *ACS Nano* **2013**, *7*, 3045-3052.
- ¹² a) P.L. Potapov, S. E. Kulkova, D. Schryvers, J. Verbeeck, *Phys. Rev. B.* **2001**, *64*, 184110; b) R. D. Leapman, L. A. Grunes, P. L. Fejes, *Phys. Rev. B.* **1982**, *26*, 614-635.
- ¹³ a) S. Liu, N. Huo, S. Gan, Y. Li, Z. Wei, B. Huang, J. Liu, J. Li, H. Chen, *J. Mater. Chem. C* **2015**, *3*, 10974-10980; b) J. Lin, L. Liang, X. Ling, S. Zhang, N. Mao, N. Zhang, B. G. Sumpter, V. Meunier, L. Tong, J. Zhang, *J. Am. Chem. Soc.* **2015**, *137*, 15511-15517; c) Y. Feng, J. Zhou, Y. Du, F. Miao, C.G. Duan, B. Wang, X. Wan, *J. Phys.: Condens. Matter* **2015**, *27*, 185302(1)-185302(6).

-
- ¹⁴ a) S. Liu, N. Huo, S. Gan, Y. Li, Z. Wei, B. Huang, J. Liu, J. Li, H. Chen, *J. Mater. Chem. C* **2015**, *3*, 10974-10980; b) J. Lin, L. Liang, X. Ling, S. Zhang, N. Mao, N. Zhang, B. G. Sumpter, V. Meunier, L. Tong, J. Zhang, *J. Am. Chem. Soc.* **2015**, *137*, 15511-15517; c) Y. Feng, J. Zhou, Y. Du, F. Miao, C.G. Duan, B. Wang, X. Wan, *J. Phys.: Condens. Matter* **2015**, *27*, 185302(1)-185302(6).
- ¹⁵ S. Yang, J. Dong, Z. Yao, C. Shen, X. Shi, Y. Tian, S. Lin, X. Zhang, *Sci. Rep.* **2014**, *4*, 4501.
- ¹⁶ H. Can, Ö. Metin, *Appl. Cat. B-Environ.* **2012**, *125*, 304-310.
- ¹⁷ M. Caporali, A. Guerriero, A. Ienco, S. Caporali, M. Peruzzini, L. Gonsalvi, *Chem. Cat. Chem.* **2013**, *5*, 2517 – 2526.
- ¹⁸ Y. Hongfeng, M. Zhen, C. Miaofang, D. Sheng, *Catal. Lett.* **2010**, *136*, 209-221.
- ¹⁹ J. Zhang, X. Jin, P. I. Morales-Guzman, X. Yu, H. Liu, H. Zhang, L. Razzari, J. P. Claverie, *ACS Nano*, **2016**, *10*, 4496-4503.
- ²⁰ G. Goncalves, P.A.A. Marques, C. M. Granadeiro, H.I.S. Nogueira, M.K. Singh, J. Grácio, *Chem. Mater.* **2009**, *21*, 4796-4802.
- ²¹ J. Park, E. Kang, S.U. Son, H. M. Park, M. K. Lee, J. Kim, K. W. Kim, H.-J. Noh, J.-H. Park, C.J. Bae, J.-G. Park, T. Hyeon, *Adv. Mat.* **2005**, *17*, 429-434.
- ²² K. E. B. Doncom, A. Pitto-Barry, H. Willcock, A. Lu, B.E. McKenzie, N. Kirby, R. K. O'Reilly, *Soft Matter* **2015**, *11*, 3666-3676.